

Resonance Raman Observation of Surface Carbonyl Groups on Carbon Electrodes Following Dinitrophenylhydrazine Derivatization

Mark A. Fryling,[†] Jun Zhao, and Richard L. McCreery*

Department of Chemistry, The Ohio State University, 120 West 18th Avenue, Columbus, Ohio 43210

Dinitrophenylhydrazine (DNPH) was used to form hydrazone derivatives of carbonyl groups on glassy carbon (GC) and pyrolytic graphite surfaces. The DNPH adducts of benzoquinone and acetone have cross sections of 488 nm, much larger than those of either DNPH or the underivatized carbonyl group. The result of this enhancement is that the Raman spectrum of DNPH-modified GC is dominated by adduct features and is not sensitive to residual adsorbed reagents. In addition, resonance Raman active adducts were not formed from DNPH reactions with model compounds containing lactone, phenol, or carboxylate groups. Assuming that the cross section of surface carbonyl adducts on GC is comparable to that of the benzoquinone adduct, the detection limit for carbonyl groups on GC is less than 1% of a monolayer. The coverage of carbonyl groups increases significantly following electrochemical oxidation of both GC and highly ordered pyrolytic graphite. Analysis of the spectra of the benzoquinone/DNPH adduct permitted assignment of prominent resonance Raman and IR features and revealed that the electrons in the hydrazone linkage are delocalized extensively.

Carbon electrodes have been used extensively in both electroanalytical and electrosynthetic applications.^{1,2} Despite the wide use of carbon electrodes, however, the rich surface chemistry and specifically the chemical nature of oxides existing at carbon surfaces have been difficult to determine in most cases.¹⁻³ Characterization of the chemical identity and local environment of surface oxides on carbon is of interest for several reasons. First, standard electrode pretreatment procedures often involve either the direct electrochemical generation of surface oxides or mechanical treatments which are likely to induce some degree of surface oxidation.⁴⁻¹¹ Second, though creation of surface oxides

may not be the primary activation mechanism for all redox couples, direct catalysis by specific surface oxide functionalities is believed to be important for electrochemical activation of some systems.^{5,7,10,11} Inner-sphere catalysis, redox mediation, proton transfer, and chemisorption have all been reported to involve oxygen-containing functional groups on carbon electrodes.¹⁰⁻¹³ It is therefore desirable to develop techniques which may qualitatively and quantitatively identify certain specific surface oxide functional groups.

A variety of surface analytical techniques have been used to characterize surface oxides on carbon, including acid/base titrations, XPS and related UHV techniques, thermal desorption mass spectrometry, electrochemistry, and optical spectroscopy.^{1,2,14-31} Derivatization with a fluorescence label was used recently to identify surface carboxylates,³² and XPS tags for carbonyl and phenol groups have been reported.^{33,34} Voltammetry of electroactive tags has been used to quantify surface groups.^{3,11,21} The results of these methods depend strongly on electrode pretreatment, but substantial data on the identity and coverage of particular oxides are available.

[†] Present address: General Mills, 15200 Industrial Park Blvd. NE, Covington, GA 30209.

- (1) Kinoshita, K. *Carbon: Electrochemical and Physicochemical Properties*; Wiley: New York 1988.
- (2) McCreery, R. L. In *Electroanalytical Chemistry*; Bard, A. J., Ed.; Marcel Dekker: New York, 1991; Vol. 17, pp 221-374.
- (3) Murray, R. C. In *Electroanalytical Chemistry*; Bard, A. J., Ed.; Marcel Dekker: New York, 1984; Vol. 13, pp 191-368.
- (4) Engstrom, R. C. *Anal. Chem.* **1982**, *54*, 2310.
- (5) Engstrom, R. C.; Strasser, V. A. *Anal. Chem.* **1984**, *56*, 136.
- (6) Hu, I. F.; Karweik, D. H.; Kuwana, T. *J. Electroanal. Chem.* **1985**, *188*, 59.
- (7) Wightman, R. M.; Deakin, M. R.; Kovach, P. M.; Kuhr, W. G.; Stutts, K. J. *J. Electrochem. Soc.* **1984**, *131*, 1578.
- (8) Fagan, D. T.; Hu, I. F.; Kuwana, T. *Anal. Chem.* **1985**, *57*, 2759.
- (9) McDermott, C. A.; Kneten, K. R.; McCreery, R. L. *J. Electrochem. Soc.* **1993**, *140*, 2593.

- (10) Cabaniss, G. E.; Diamantis, A. A.; Murphy, W. R.; Linton, R. W.; Meyer, T. *J. Am. Chem. Soc.* **1985**, *107*, 1845.
- (11) Karweik, D. H.; Hu, I. F.; Weng, S.; Kuwana, T. In *Catalyst Characterization Science: Surface and Solid State Chemistry*; Deviney, M. L., Gland, J. L., Eds.; ACS Symposium Series 288; American Chemical Society: Washington, DC, 1985.
- (12) Nagaoka, T.; Yoshino, T. *Anal. Chem.* **1986**, *58*, 1037.
- (13) Barbero, C.; Juana, J. S.; Leonides, S. *J. Electroanal. Chem.* **1988**, *248*, 321.
- (14) Donnet, J. B. *Carbon* **1968**, *6*, 161.
- (15) Boehm, H. P. *Adv. Catal.* **1964**, *16*, 179.
- (16) Barton, S. S.; Boulton, G. L.; Harrison, B. H. *Carbon* **1972**, *10*, 395.
- (17) Panzer, R. E.; Elving, P. J. *Electrochim. Acta* **1975**, *20*, 635.
- (18) Kamau, G. N.; Willis, W. S.; Rusling, J. F. *Anal. Chem.* **1985**, *57*, 545.
- (19) Bowers, M. L.; Hefter, J.; Dugger, D. L.; Wilson, R. *Anal. Chim. Acta* **1991**, *248*, 127.
- (20) Wandass, J. H.; Gardella, J. A.; Weinberg, N. L.; Bolster, M. E.; Salvati, L. *J. Electrochem. Soc.* **1987**, *134*, 2734.
- (21) Elliott, C. M.; Murray, R. W. *Anal. Chem.* **1976**, *48*, 1247.
- (22) Kozlowski, C.; Sherwood, P. M. A. *J. Chem. Soc., Faraday Trans. 1* **1984**, *80*, 2099.
- (23) Kozlowski, C.; Sherwood, P. M. A. *J. Chem. Soc., Faraday Trans. 1* **1985**, *81*, 2745.
- (24) Harvey, J.; Kozlowski, C.; Sherwood, P. M. A. *J. Mater. Sci.* **1987**, *22*, 1585.
- (25) Fagan, D. T.; Kuwana, T. *Anal. Chem.* **1989**, *61*, 1017.
- (26) Drushel, H. V.; Hallum, J. V. *J. Phys. Chem.* **1958**, *62*, 1502.
- (27) Blurton, K. F. *Electrochim. Acta* **1973**, *18*, 869.
- (28) Schreurs, J.; van den Berg, J.; Wonders, A.; Barendrecht, E. *Recl. Trav. Chim. Pays-Bas* **1984**, *103*, 251.
- (29) Porter, M. D.; Bright, T. B.; Allara, D. L.; Kuwana, T. *Anal. Chem.* **1986**, *58*, 2461.
- (30) Kepley, L. J.; Bard, A. J. *Anal. Chem.* **1988**, *60*, 1459.
- (31) Barbero, C.; Kötzt, R. *J. Electrochem. Soc.* **1993**, *140*, 1.
- (32) Pantano, P.; Kuhr, W. G. *Anal. Chem.* **1991**, *63*, 1413.
- (33) Collier, W. G.; Tougas, T. P. *Anal. Chem.* **1987**, *59*, 396.
- (34) Tougas, T. P.; Collier, W. G. *Anal. Chem.* **1987**, *59*, 2269.

Vibrational spectroscopy is attractive for characterizing carbon oxides because IR and Raman spectra are quite sensitive to the nature of the oxide present. In principle, it should be possible to distinguish carbonyl groups from phenols, ethers, etc., as well as to infer structural differences between one carbonyl site and another. The level of structural information available from vibrational spectroscopy should be higher than that obtained by XPS or fluorescence methods, assuming that good quality spectra are available. Unfortunately, vibrational spectra of carbon surface oxides have been obtained only for high surface area carbon materials which are difficult to characterize electrochemically.¹ The weakness of a surface selection rule for IR absorption at carbon has prevented acquisition of spectra from monolayers on carbon electrodes.²⁹ Surface enhancement of Raman scattering is unknown and unlikely on carbon surfaces, and oxygen functional groups are weak Raman scatterers to begin with. The high surface area carbons for which IR spectra are available are not useful for most electroanalytical purposes and are not amenable to the variety of pretreatments in common use for glassy carbon and pyrolytic graphite.

The present report discusses a probe of carbonyl density on carbon surfaces based on resonance Raman spectroscopy. Dinitrophenylhydrazine (DNPH) is a specific reagent for ketone and aldehyde groups which leads to a resonance Raman active product. After establishing that DNPH reacts with surface carbonyl groups, the surface spectra were analyzed to determine the structure of the adduct, and the carbonyl coverage was estimated.

EXPERIMENTAL SECTION

Materials. Glassy carbon electrodes (GC20s) were either purchased as a complete electrode (Bioanalytical Systems) or were constructed from 1 mm thick GC20 plate (Tokai, Japan). Glassy carbon (GC) was polished on a Microcloth polishing cloth using successive 1.0, 0.3, and 0.05 μm alumina (Buehler). The dry alumina was slurried with NANOpure 18 M Ω water (Barnstead), and the electrode was rinsed and sonicated between polishing steps with NANOpure. Highly ordered pyrolytic graphite (HOPG) was a gift from Arthur Moore at Union Carbide Corp. HOPG surfaces were prepared by cleaving the basal plane using adhesive tape.

2,4-Dinitrophenylhydrazine was used as purchased (J. T. Baker) in a 10 mM solution with 1% HCl (J. T. Baker) in absolute ethanol (Quantum Chemical). Model molecules were all used as received and included benzophenone (Fisher), *p*-benzoquinone (MCB), phenanthrenequinone, 1,2-naphthoquinone, 1,4-naphthoquinone, 2-hydroxy-1,4-naphthoquinone, 5,8-dihydroxy-1,4-naphthoquinone, 9-fluorenone, coumarin, phenol, and benzoic acid (all from Aldrich).

Instrumentation. Electrochemical pretreatment was performed using a PAR 173 potentiostat. The potentiostat output was monitored using a V to F converter and a pulse counter (Hewlett Packard) so that total charge passed during anodization could be monitored. Oxidation of the carbon working electrode was carried out in an all-glass cell containing 1 M H₂SO₄, a Pt auxiliary, and a Ag/AgCl (3 M KCl) reference electrode (BAS). The potential was stepped to 2.2 V and held for 10 s unless stated otherwise.

Raman experiments were conducted using a custom spectrometer as shown in Figure 1. The spectrograph was a 640 mm, *f*/5.6 single stage monochromator (Instruments SA) containing a single grating with 600 lines/mm blazed at 500 nm. A PM512 CCD (Photometrics) was used for detection. The focusing/collection

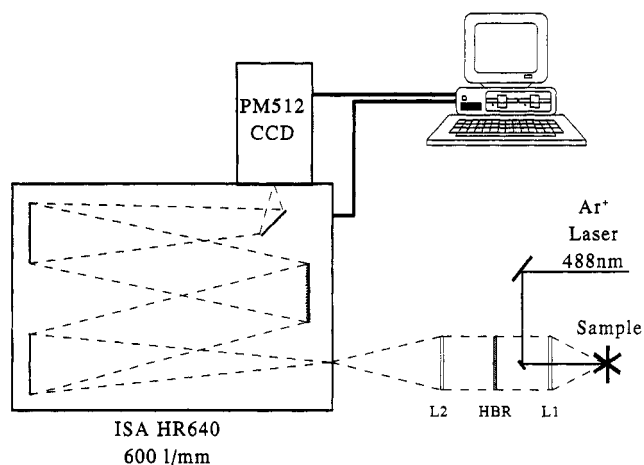


Figure 1. Block diagram of spectrometer, showing 180° illumination optics. Ar⁺ laser was filtered by a 488 nm interference filter; L1 had a 120 mm focal length.

lens was 40 mm in diameter, *f*/2.5, and the lens focusing onto the monochromator entrance slit was also 40 mm in diameter but *f*/5. A 38 mm diameter, 488 nm holographic band rejection filter (Notch+, Kaiser Optical Systems) was used in the collimated region. The entrance slit width was 49 μm for a resolution of approximately 4 cm^{-1} . Excitation was carried out using the 488 nm line of an Argon ion laser (Coherent Innova 70) with a power of approximately 10 mW at the sample focused to a 60 μm diameter spot size.

Procedures. Model adduct molecules were made by addition of 1×10^{-5} mol of the model compound to 100 mL of dry ethanol containing 1×10^{-5} mol of DNPH and 1% HCl. Reactions occurred rapidly, as evidenced by color change. Typically the reaction products were orange to red in color. If an insoluble precipitate was formed, the solution was filtered, and both the filtrate and the supernatant liquid were examined spectroscopically. In order to "force" the azo form of the adduct, a fraction of each product was treated with 0.1 M KOH in dry ethanol until a color change was observed. The resulting product was then examined spectroscopically.

Carbon samples were pretreated by various means prior to reaction with DNPH. GC surfaces were polished and in some cases electrochemically pretreated before reacting with DNPH. In the case of HOPG, fresh basal plane was exposed by cleaving, and the surface was then either examined as is or electrochemically pretreated prior to analysis. The DNPH reaction protocol for the carbon samples involved immersing the carbon surface in a solution containing 10 mM DNPH in dry ethanol containing 1% HCl. The DNPH solution was deoxygenated prior to use by saturation with argon for 20 min. The DNPH solution with the immersed carbon sample was then heated to its boiling point (about 75 °C). The heat was then turned off, and the electrode was allowed to continue soaking in the solution with stirring for a total contact time of 2 h. After the 2 h DNPH treatment, the electrode was removed from the solution and rinsed carefully with dry ethanol. Unless otherwise noted, the electrode was then soaked for 5 min in a solution containing 0.1 M KOH in absolute ethanol. Following this treatment, the electrode was removed from the KOH solution, rinsed again with absolute ethanol, and carefully dried in a stream of argon gas. The electrode was then analyzed spectroscopically.

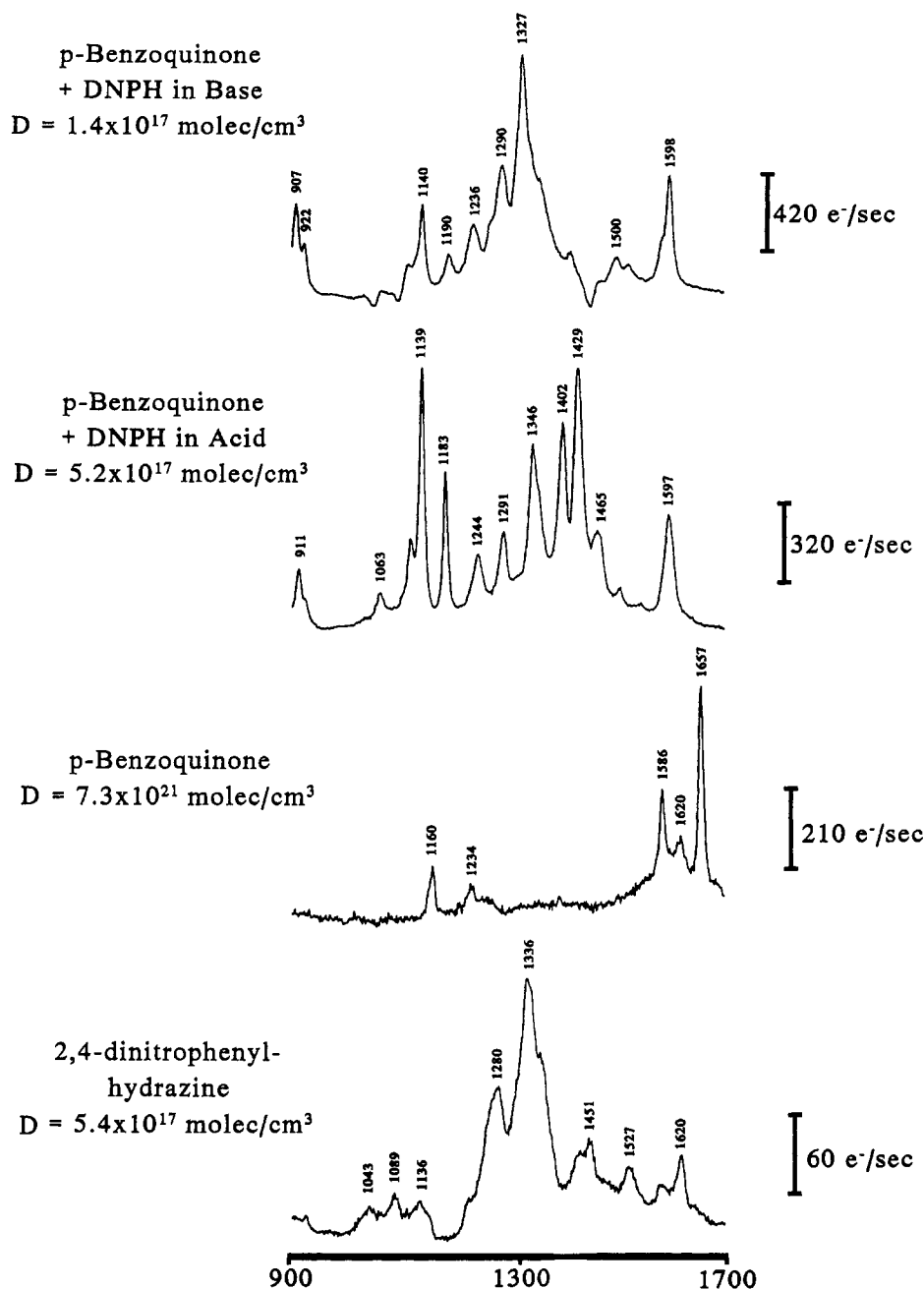


Figure 2. Raman spectra of solutions of the materials indicated. Laser power at sample was 10 mW, focused to a 60 μm diameter beam waist.

RESULTS AND DISCUSSION

Qualitative Features of DNPH Adducts. Raman spectra of the reagents and the product of the DNPH reaction with benzoquinone (BQ) are shown in Figure 2. Note that the number density of the adduct is much smaller than that of the reagents, indicating that the resonance-enhanced adduct is a much stronger scatterer. Under the conditions employed in Figure 2, the adduct cross section is about 4×10^4 larger than benzoquinone and 27 times larger than DNPH. Although DNPH is considered a specific reagent for aldehyde and ketone carbonyl groups, attempts were made to form adducts from phenol, coumarin (a lactone), and benzoic acid. Under identical reaction and spectroscopic conditions, DNPH derivatives of coumarin, phenol, and benzoic acid were too weak to be observed, while benzoquinone yielded the strong resonance Raman spectrum shown in Figure 2. Although the DNPH reagent did exhibit a 1336 cm^{-1} feature which was

much weaker than that of the BQ/DNPH adduct, the DNPH decomposed in base, completely removing its spectral features. As will be shown below, the adducts of DNPH with BQ and surface carbonyls are stable in acid and base.

The basal plane of HOPG has a very low density of edge sites where oxides can exist, so a reaction between DNPH and HOPG should yield a very low density of resonance Raman active adducts. Figure 3A shows an HOPG basal plane spectrum after DNPH treatment. DNPH treatment has no effect on the basal plane spectrum, implying that the number density of the adduct is below the detection limit for the native basal plane. Electrochemical oxidation of the basal plane yielded spectrum B of Figure 3. The E_{2g} band broadened, and the "D" band at 1360 cm^{-1} is apparent, indicating disordering of the graphite lattice by the ECP.^{35,36}

(35) Tuinstra, F.; Koenig, J. L. *J. Chem. Phys.* **1970**, *53*, 1126.

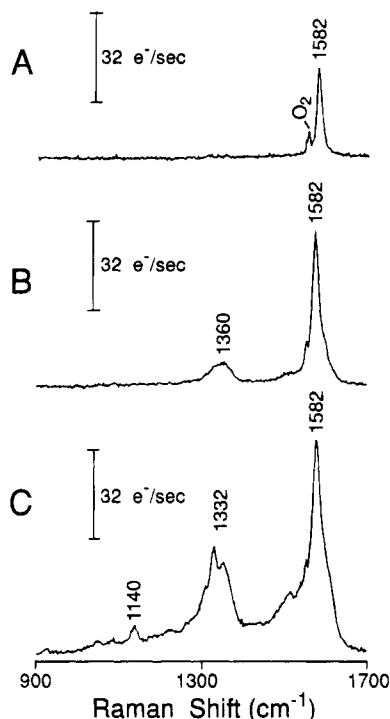


Figure 3. Raman spectra of HOPG basal plane, 10 mW laser power in air, 300 s integration. (A) Freshly cleaved and then DNP treated. (B) Freshly cleaved, followed by 10 s ECP at 2.2 V in 1.0 M H₂SO₄. (C) After ECP and DNP treatment. The small feature on the side of the E_{2g} graphite peak is atmospheric oxygen.

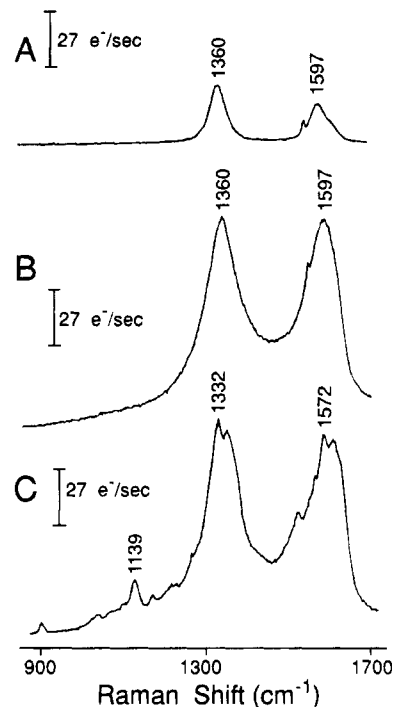


Figure 5. Raman spectra of GC preceding (A) and following (B) ECP (2.2 V, 10 s, in 1 M H₂SO₄). Spectrum C is the same sample as was used for spectrum B, following DNP treatment. Note that all three spectra have the same intensity scale.

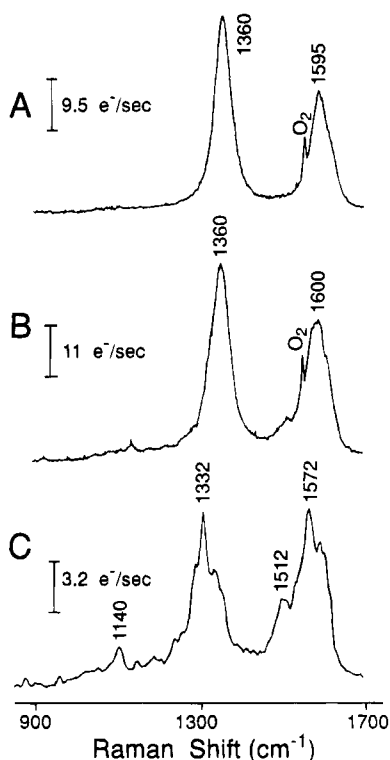


Figure 4. Raman spectra of polished GC, 10 mW laser power, 300 s integration. (A) Polished surface. (B) After DNP treatment. (C) Difference of spectra B and A.

Derivatization of the electrochemically pretreated surface with DNP leads to small Raman features at 1139 and 1332 cm⁻¹, apparent in spectrum C of Figure 3. As will be shown below, the

1139 cm⁻¹ band is attributable to an N–N stretch in the GC/DNP adduct, while the 1332 cm⁻¹ band is the dinitrophenyl–N stretch.

Glassy carbon is an isotropic material on distance scales greater than about 1000 Å, with a high density of edge sites on any exposed surface.² Figure 4 shows Raman spectra of polished GC before (A) and after (B) DNP treatment. Figure 4C is the GC/DNP spectrum remaining after the spectrum 4A was subtracted from 4B. The features at 1140 and 1332 cm⁻¹ are increased in size if the GC is oxidized before DNP treatment, as noted below. For a GC surface which had been sputtered by Ar⁺ ions in UHV (<10⁻⁸ Torr), fast air transfer to the DNP reagent solution yielded no observable 1140 or 1332 cm⁻¹ Raman peaks.

Electrochemical pretreatment (ECP) of the GC surface is known to increase the O/C ratio as determined by XPS.^{5,10,12,22–24} Figure 5 shows spectra from the same piece of GC before oxidation (A), after 10 s at 2.2 V vs Ag/AgCl in 1.0 M H₂SO₄ (B), and again after DNP derivatization (C). Comparison of spectra A and B shows the increase in Raman intensity with ECP reported previously, which presumably arises from an increase in sampling depth in the partially transparent oxidized carbon layer.^{36,37} Kepley and Bard have reported small graphitic carbon particles in the oxidized film, and these may be responsible for the increase in the Raman signal.³⁰ The features derived from DNP (particularly those at 1140 and 1332 cm⁻¹) have higher intensities for the electrochemically pretreated surface compared to the polished surface. Figure 6 compares spectra of electrochemically pretreated and DNP-treated surfaces which were acid treated (A) and base treated (B) following derivatization, with the carbon features subtracted. The 1140, 1332, and 1500–1600 cm⁻¹ features

(36) Bowling, R.; Packard, R. T.; McCreery, R. L. *Langmuir* 1989, 5, 683.

(37) Alsmeyer, Y. W.; McCreery, R. L. *Langmuir* 1991, 7, 2370.

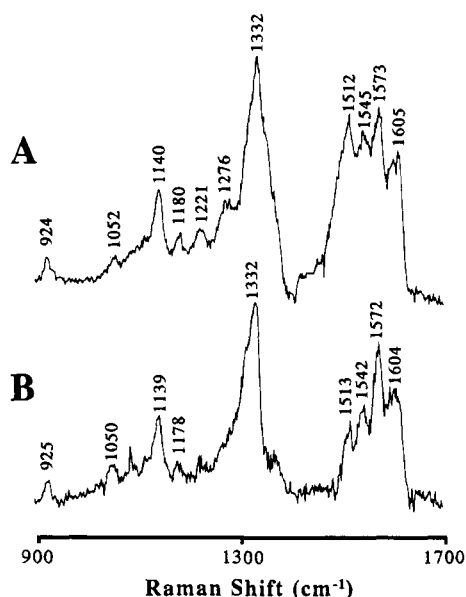
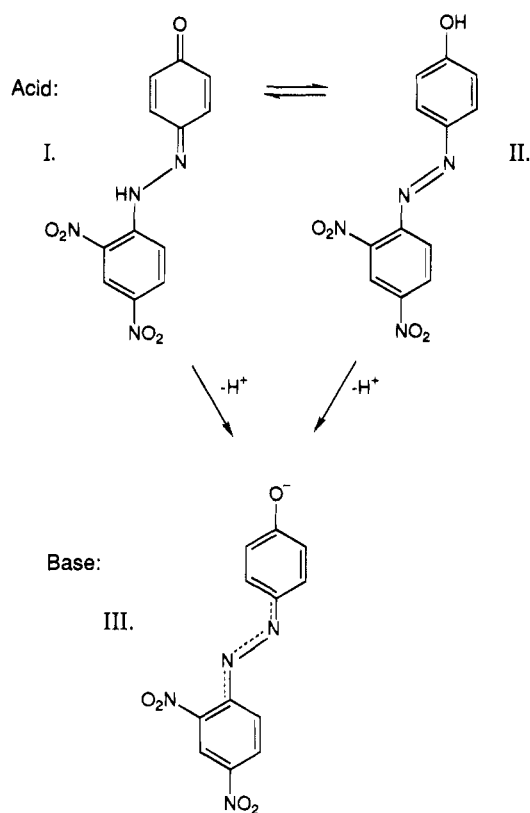


Figure 6. Spectra of GC after ECP and DNPH treatment, following acid (A) and base (B) washes. Carbon spectra preceding DNPH treatment were subtracted, so features shown arose during DNPH treatment.

Scheme 1.



are prominent on surfaces following immersion in both acid and base solutions and increase significantly in intensity for GC surfaces which had undergone additional surface oxidation.

Spectrum Interpretation. DNPH adducts of carbonyl species exhibit a variety of acid/base and tautomerization equilibria.^{38–48}

(38) Trotter, P. J. *Appl. Spectrosc.* **1977**, *31*, 30.

(39) Jacques, P. J. *Raman Spectrosc.* **1982**, *12*, 102.

(40) Morgan, K. J. *J. Chem. Soc.* **1961**, 2151.

(41) Drozdowski, P. M. *Spectrochim. Acta* **1985**, *41A*, 1035.

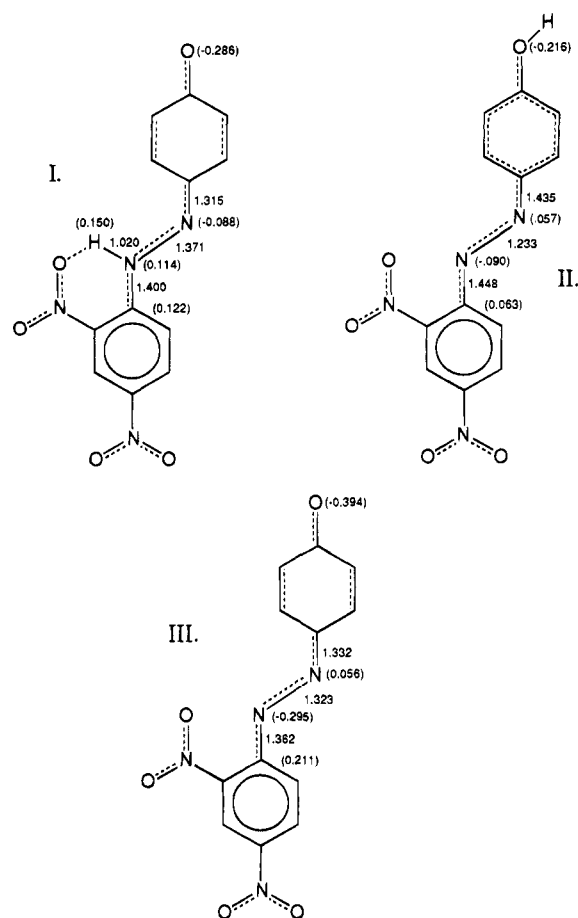


Figure 7. Bond lengths and partial charges (in parentheses) calculated by Hyperchem for three forms of the BQ/DNPH adduct. Only the variables which change significantly upon protonation are shown, to improve clarity.

The case of benzoquinone was chosen as a model, mainly because of the similarity of the BQ/DNPH adduct spectrum and the GC/DNPH spectrum in base. The protonated form present in acid can exist in at least the two forms shown in Scheme 1, one of which contains the azo group (structure II). In base, loss of H⁺ leads to a molecule with several resonance forms, one of which is shown in Scheme 1 (structure III).

In acid, the BQ/DNPH spectrum (Figure 2) has several features expected for structure II and is similar to that of Trotter for phenylazophenol in acid.³⁸ The prominent 1429 cm⁻¹ band in the DNPH/BQ adduct spectrum has been attributed to the N=N stretch³⁸ and is absent in the IR, as expected. The 1139 cm⁻¹ band could be the C–N stretch of structure II or the N–N stretch of structure I. Given the strength of the 1138 cm⁻¹ band in the IR and the prominence of the N=N stretch in the acid spectrum, the likely structure of the DNPH/BQ adduct in acid is structure

(42) Barnes, A. J.; Majid, M. A.; Stucker, M. A.; Gregory, P.; Stead, C. V. *Spectrochim. Acta* **1985**, *41A*, 629.

(43) Machida, K.; Kim, B.-K.; Saito, Y.; Igarashi, K.; Uno, T. *Bull. Chem. Soc. Jpn.* **1974**, *47*, 78.

(44) Saito, Y.; Kim, K.-B.; Machida, K.; Uno, T. *Bull. Chem. Soc. Jpn.* **1974**, *47*, 2111.

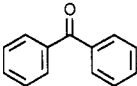
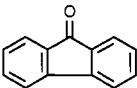
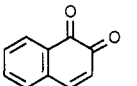
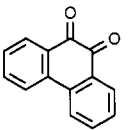
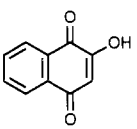
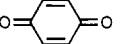
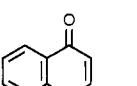
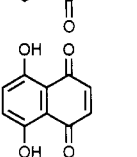
(45) Monohan, A. R.; DeLuca, A. F.; Ward, A. T. *J. Org. Chem.* **1971**, *36*, 3838.

(46) Morresi, A.; Paliani, P.; Santini, S.; Cataliotti, R. S. *Can. J. Spectrosc.* **1988**, *33*, 69.

(47) Cataliotti, R. S.; Morresi, A.; Paliani, G.; Zgierski, M. Z. *J. Raman Spectrosc.* **1989**, *20*, 601.

(48) Chattopadhyay, S.; Kasta, G. S.; Brahma, S. K. *J. Raman Spectrosc.* **1991**, *22*, 449.

Table 1. Observed Raman Bands for Carbonyl/DNPH Derivatives

model molecules	conditions	adduct Raman bands (cm ⁻¹) ^c			
		N—N (I, ν_{51} ; III, ν_{51})	Ph—N (I, ν_{65} ; III, ν_{60})	C=N (I, ν_{67} ; III, ν_{65})	other strong Raman bands
	acidic ^a basic ^b	1134 (s)	1335 (s) 1327 (s)	1602 (vs)	1280, 1362, 1616 919, 1364, 1440, 1472
	acidic basic	1132 (vs)	1356 (vs) 1338 (s)	1603 (s)	1275, 1314, 1583, 1620 920, 1022, 1453, 1544
	acidic basic	1151 (w) 1149 (s)	1312 (s) 1327 (vs)	1607 (s) 1607 (s)	984, 1197, 1347, 1553 923, 969, 1029, 1557
	acidic basic	1130 (w) 1125 (m)	1337 (m) 1340 (s)	1598 (s) 1598 (s)	921, 960, 1194, 1576 964, 1049, 1225, 1500
	acidic basic	1144 (w) 1140 (w)	1340 (m) 1331 (m)	1603 (s) 1603 (s)	986, 923, 1520, 1561 923, 986, 1520, 1561
	acidic basic	1139 (vs) 1140 (s)	1346 (s) 1331 (vs)	1597 (s) 1598 (s)	910, 1183, 1402, 1430 910, 1190, 1236, 1290
	acidic basic	1142 (w)	1332 (m) 1314 (m)	1598 (m) 1600 (w)	923, 1175, 1362, 1518 923, 980, 1364, 1420
	basic	1134 (s)	1354 (w)	1603 (s)	920, 1045, 1223

^a Final wash before spectroscopy was 0.1 M HCl in ethanol. ^b Final wash before spectroscopy was 0.1 M KOH in ethanol. ^c Subscripts on ν are Wilson numbers for modes shown in Figure 8.

II of Scheme 1. In basic solution, the complete absence of an azo stretch indicates that an N=N double bond is unlikely in structure III, but rather the adduct exists as a different resonance form. Prediction of the electronic structure and vibrational modes for the structures in Scheme 1 was assisted by a commercial molecular mechanics program Hyperchem (release 3, Autodesk, Inc.) and comparison to literature assignments.³⁸⁻⁴⁸ Although computer calculations are not expected to yield accurate vibrational frequencies, they can help predict trends and assign bands to normal modes. The DNPH/BQ adduct structure was first optimized using the semiempirical PM3 procedure, yielding the structures of Figure 7. Structure I, formed in acid, is protonated at the nitrogen adjacent to the dinitrophenyl ring, and hydrogen bonding occurs between the proton and the ortho NO₂ group. The calculated bond length for the hydrazone C=N bond is 1.315 Å, comparable to C=N double bonds, while the N—N bond length is 1.371 Å, quite long for an N—N double bond. Structure II is a tautomer of I, with its shorter N=N bond (1.233 Å) implying a true azo structure. When the benzoquinone adduct is in base, the loss of a proton yields an anion (structure III). The negative charge is delocalized over the dinitrophenyl ring and N—N linkage, implying extensive conjugation of the Ph—N—N—C backbone. The N—N bond length decreases to 1.323 Å, and the dinitrophenyl—N bond decreases to 1.362 Å. These results are consistent

with delocalization of the anion following deprotonation, with a shift from a hydrazone structure with a C=N double bond in acid to a delocalized structure with partial double bonds along the C—N—N—C linkage in base.

Calculation of vibrational modes for the benzoquinone adduct is nontrivial, since at least 78 modes are involved, and band assignments should be considered tentative. Several relevant vibrational modes of structures I–III are illustrated in Figure 8. The 1429 cm⁻¹ Raman band observed in acid is assigned to the N=N stretch, ν_{71} . In base, the corresponding mode (ν_{51} of structure III) is at lower frequency due to weakening of the N—N bond. Stated qualitatively, the 1429 cm⁻¹ mode is primarily an azo stretch in acid but becomes a single N—N bond stretch (1140 cm⁻¹) in base. The strong 1327 cm⁻¹ feature observed for DNPH/BQ and GC/DNPH in base is likely to be ν_{60} , structure III. The bands in the region of 1600 cm⁻¹ are associated with the phenyl ring and the hydrazone stretch (I, ν_{67} ; III, ν_{65}). To assess the effect of carbonyl structure on the adduct spectrum, a variety of model compounds were derivatized and examined spectroscopically. As shown in Table 1, peaks with Raman shifts corresponding to the ν_{51} , ν_{65} , and ν_{67} modes were observed for a large number of hydrazones, although there are significant differences in relative intensities. Table 2 lists observed and calculated vibrational modes for the benzoquinone spectra. Hyperchem often predicts

Table 2. Assignments of Observed and Calculated Vibrational Modes

structure	<i>p</i> -benzoquinone					GC/ECP Raman <i>f</i> (cm ⁻¹), <i>I</i>	polished GC Raman <i>f</i> (cm ⁻¹), <i>I</i>	HOPG/ECP Raman <i>f</i> (cm ⁻¹), <i>I</i>
	Raman ^a	IR ^a	Hyperchem calcd					
	<i>f</i> (cm ⁻¹), <i>I</i>	<i>f</i> (cm ⁻¹), <i>I</i>	mode ^b	<i>f</i> (cm ⁻¹)	<i>I</i> (IR)			
I	911, m	906, m	40	906	m			
	918, w	918, m	41	935	m	924, w		
	1139, vs	1138, vs	51	1184	vs	1140, m		
	1183, s	1184, m	56	1322	s	1180, w		
	1291, m	1286, m	57	1348	s	1276, w		
	1346, s,b		65	1612	w	1332, s		
		1348, vs,b	64	1590	vs			
	1597, s,b		67	1773	w	1605, s		
		1602, vs	68 ^c	1785	s			
	II	1139, s	1138, vs	53	1232	w		
1402, vs		1400, m						
1429, vs		1424, m	71	1885	w			
		1602, vs	67 ^c	1760	s			
III	907, s	908, m	40	954	s			
	922, m	924, w	43	997	s	925, w	925, w	924, w
	1140, s	1136, vs	51	1216	vs	1139, m	1141, m	1139, m
	1190, m	1192, s	55	1325	vs	1178, w	1181, w	
	1290, s	shld, s	57	1416	s		1269, m	
		1298, s,b						
	1327, vs,b	shld, s	60	1545	s	1332, s	1334, s	1333, s
		1344, s,b	61	1562	vs			
		1586, s,b						
	1598, s	shld, s	65	1715	s	1604, s		

^a w, weak; m, medium; s, strong; vs, very strong; shld, shoulder; b, broad. ^b Wilson number for normal modes; several are illustrated in Figure 8. ^c Benzene ring deformation.

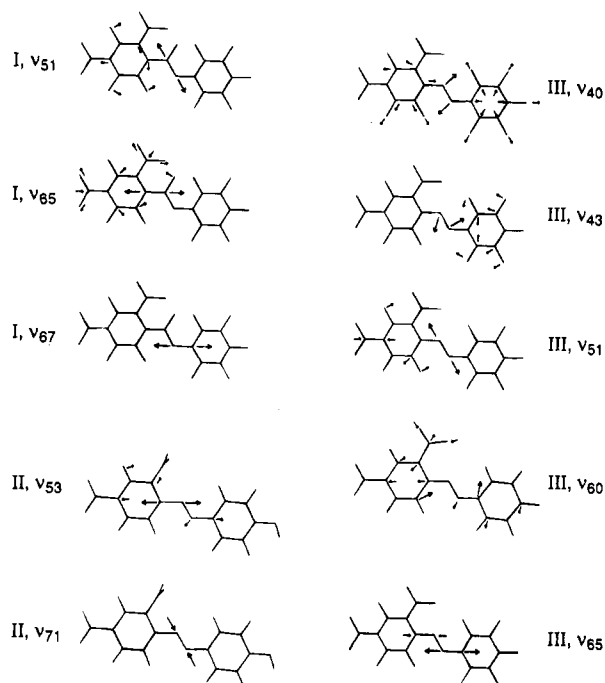


Figure 8. Vibrational modes predicted by Hyperchem for structure I (acid) and structure III (deprotonated). The left ring is the dinitrophenyl ring; the right ring is the quinone. Subscripts denote Wilson numbers for modes listed in Table 2. Larger arrows indicate greater atomic motion.

vibrational frequencies which are about 10% higher than observed, but the consistency of the predicted and observed IR intensities increases our confidence in the assignment.⁴⁹ The mode frequencies for the GC spectra were not calculated but were assigned to

modes by analogy to the BQ/DNPH features. The IR and Raman spectra for the benzoquinone derivative are compared in Figure 9 for the acid and base forms. Notice the prominent bands at 1140, 1327, and 1598 cm⁻¹. The frequencies in the IR and Raman spectra do not correspond exactly because certain bands (e.g., 1327 cm⁻¹) are composed of several modes with similar frequencies but different IR and Raman intensities. The similarity of the prominent modes at ca. 1140, 1330, and 1600 cm⁻¹ for the DNPH derivatives of GC and the model compounds of Table 1 indicates that these modes are observed for carbonyl groups in a variety of environments but not for phenolic, carboxylate, or lactone groups. To reiterate, the three modes common to DNPH/GC and many other DNPH derivatives in base correspond to the N–N stretch at ca. 1140 cm⁻¹ (III, ν₅₁), a nitrophenyl ring deformation at ca. 1330 cm⁻¹ (III, ν₆₀), and a C–N–N–C linkage stretch at ca. 1600 cm⁻¹ (III, ν₆₅).

The strong 1429 cm⁻¹ band for the DNPH/BQ adduct in acid and the similarity to several features reported by Trotter for phenylazophenol⁴² support the conclusion that structure II is the dominant form of DNPH/BQ in acid. When structure II is deprotonated in base, several resonance forms could exist, but structure III of Figure 7 is the most consistent with observations. The lack of any features in the 1400 cm⁻¹ region implies that the N=N bond has lost its azo character, and Hyperchem indicates a weaker bond (1.323 Å vs 1.233 Å). As shown in Figure 6, the DNPH/GC adduct does not exhibit the same sensitivity to pH as the BQ adduct, and an azo feature in the region of 1400 cm⁻¹ is not observed at any pH considered. There are some small changes in the 1512–1573 cm⁻¹ region with pH, but the main bands at 1139 and 1332 cm⁻¹ are not sensitive to pH. These observations imply a structure similar to that of Figure 10, with a delocalized anion similar to the deprotonated DNPH/BQ adduct. The spectra indicate that unlike the BQ adduct, the DNPH/GC

(49) Seeger, D. M.; Korzeniewski, C.; Kowalchuk, W. J. *Phys. Chem.* **1991**, *95*, 1991.

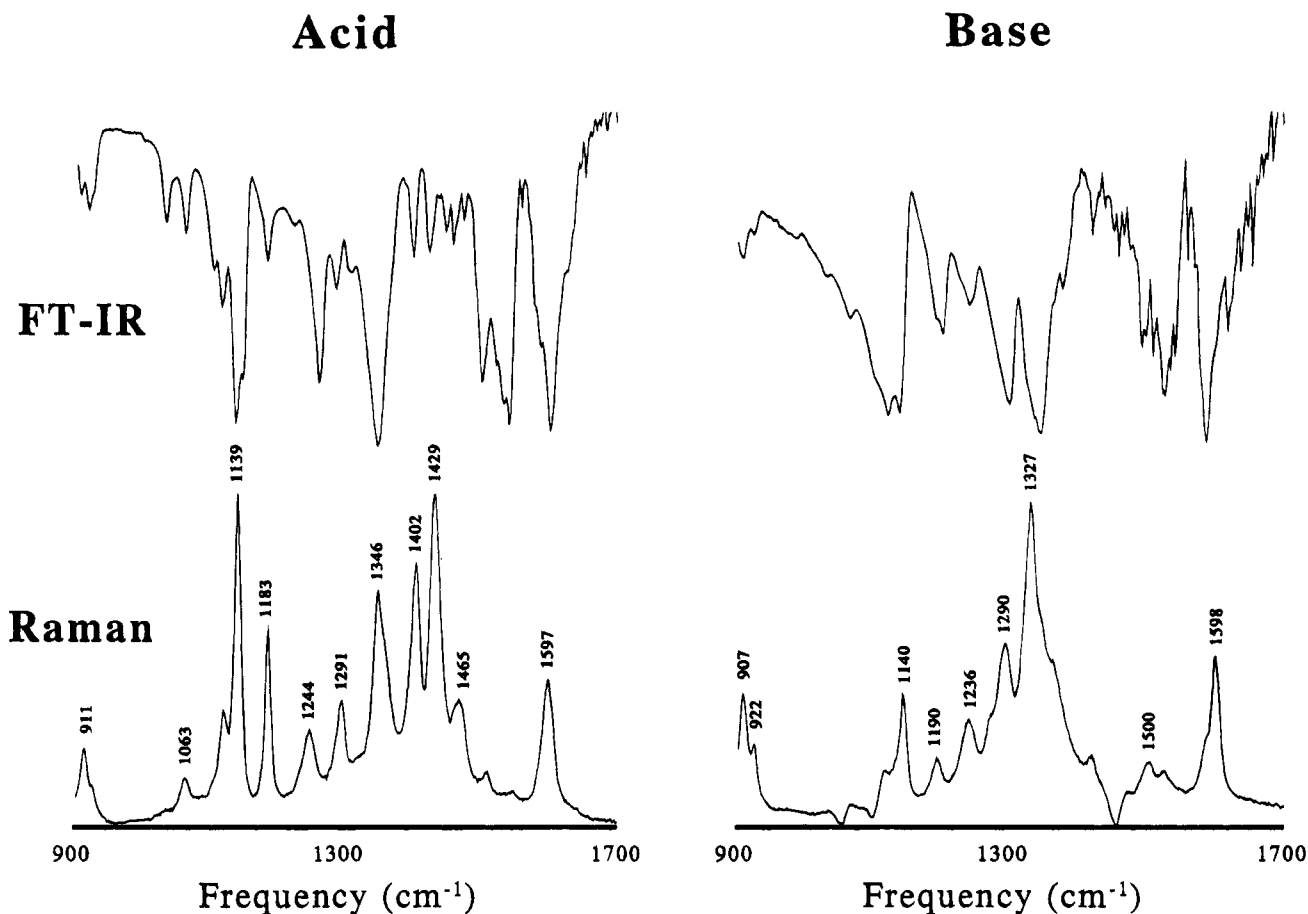


Figure 9. Observed FT-IR and Raman spectra of the BQ/DNPH solution (for Raman) and the precipitated solid (for FT-IR). IR frequencies are listed in Table 2.

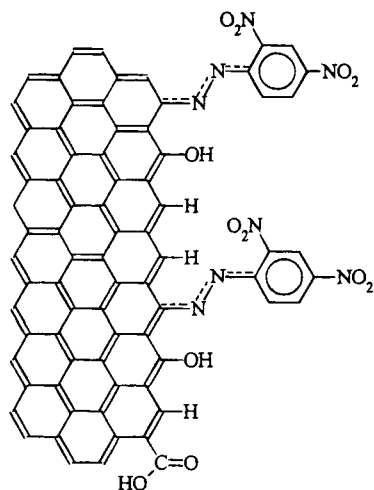


Figure 10. Proposed structure of DNPH/GC adduct. Dashed line denotes a delocalized anion extending over the C-N-N-Ph linkage.

structure does not protonate in acid. Delocalization of the anion into the carbon aromatic system may make the GC/DNPH a much weaker base than BQ/DNPH, or GC/DNPH may not protonate because of the lack of an aromatic carbonyl group.

Quantitative Determination of Carbonyl Coverage. In order to quantitatively assess carbonyl coverage, it was first necessary to determine the reproducibility and accuracy of the procedure. The expected Raman signal from a surface is given by eq 1, under the assumption that the spectrometer entrance slit and collection angle are overfilled:⁵⁰

$$S = P_D \beta D_S A_D \Omega T Q t \quad (1)$$

where S is the signal integrated over the Raman bandwidth (e^-), P_D is the laser power density at sample ($\text{photons s}^{-1} \text{cm}^{-2}$), β is the Raman cross section for the vibrational mode ($\text{cm}^2 \text{molecule}^{-1} \text{sr}^{-1}$), D_S is the surface number density of analyte (molecules cm^{-2}), A_D is the sample area observed (cm^2), Ω is the spectrometer collection angle (sr), T is the spectrometer transmission efficiency (unitless), Q is the detector quantum efficiency (e^-/photon), and t is the observation time per resolution element (s). Repeated placement of a thin cell (1 mm path length) containing benzene ($\beta = 2 \times 10^{-29} \text{cm}^2 \text{molecule}^{-1} \text{sr}^{-1}$ at 992cm^{-1})⁵¹ at the sample position shown in Figure 1 yielded a signal of $1.75 \times 10^5 \pm 7 \times 10^2 e^- \text{s}^{-1}$ ($N = 3$) for 10 mW of laser power. The predicted signal for independently measured values of A_D , Ω , T , Q , and D_S determined by the product of the number density of liquid benzene and a depth of field of 1 mm was $1.43 \times 10^5 e^- \text{s}^{-1}$. While the comparison of measured and predicted signals is not exact, it indicates that the variables of eq 1 are all accounted for. The importance of the benzene calibration for the present work is the reproducibility of 0.4% for repeated sample positioning.

When polished GC was repeatedly placed at the sample position under the same conditions, S was $737 \pm 35 e^- \text{s}^{-1}$ ($N = 3$). This value is integrated over both the 1360cm^{-1} band profile and the penetration depth of the laser (ca. 200Å) and is valid only at 488nm . For both the 1 mm path length of benzene (which

(50) Fryling, M.; Frank, C. J.; McCreery, R. L. *Appl. Spectrosc.* **1993**, *47*, 1965.

(51) Harmon, P. A.; Asher, S. A. *J. Chem. Phys.* **1990**, *93*, 3094.

is less than the depth of field of the collection optics) and the 200 Å sampling depth of GC, the use of eq 1 is conceptually equivalent to compressing the scatterers in the sampling depth to a single layer of density D_s . The Raman cross section of the BQ/DNPH adduct in base was determined by comparing the integrated intensity of the 1140 cm^{-1} band to that of the benzene 992 cm^{-1} band, which has a known cross section.⁵¹ The integrated intensity is proportional to βD for both benzene and the BQ/DNPH adduct after the spectrum is corrected for instrumental response.⁵⁰ By this procedure, the deprotonated BQ/DNPH adduct was determined to have an integrated cross section for the 1140 cm^{-1} band excited by 488 nm equal to $7.0 \times 10^{-26} \text{ cm}^2 \text{ molecule}^{-1} \text{ sr}^{-1}$. The background for GC from all other sources is $2.8 \pm 0.5 \text{ e}^- \text{ s}^{-1}$ ($N = 4$) at 1140 cm^{-1} , while a monolayer of structure III, Figure 7 ($3 \times 10^{14} \text{ molecule cm}^{-2}$), would be predicted to yield $270 \text{ e}^- \text{ s}^{-1}$ under the same conditions. Thus a signal to noise ratio of 3 should be attainable with substantially less than a monolayer of DNPH adduct.

Assuming that the cross section for the 1140 cm^{-1} band of the DNPH/GC20 adduct is equal to that for the DNPH/BQ adduct, eq 1 may be used to calculate the coverage of DNPH adducts from the 1140 cm^{-1} intensity. For $A_D = 1.3 \times 10^{-5} \text{ cm}^2$, $TQ = 0.025$, $t = 300 \text{ s}$, $P_D = 8.7 \times 10^{20} \text{ photons cm}^{-2} \text{ s}^{-1}$, and $S = 8 \times 10^3 \text{ e}^-$, the calculated D_s is $5.3 \times 10^{13} \text{ molecules/cm}^2$. Based on the approximation that polished GC has a density of carbon atoms similar to that of graphite ($4.5 \times 10^{14} \text{ carbon atoms/cm}^2$), about 1.2% of the carbon atoms on the polished surface have carbonyl groups available for reaction with DNPH. This value compares to 5%¹⁰ determined from deconvolution of the XPS C_{1s} peak and 1.4–2.8% determined from derivatization with an XPS label.³⁴

CONCLUSIONS

In summary, the DNPH derivatization leads to a high Raman cross section, which permits detection of derivatized carbonyl groups at levels of <1% of a monolayer. The reaction was selective for carbonyl groups, and Raman observable products were not obtained for a model carboxylate, lactone, or phenol. 1140, 1332, and 1600 cm^{-1} Raman modes are present in GC derivatized with DNPH and in the derivatives of most model carbonyl compounds examined in base. The spectra of DNPH-derivatized GC are consistent with electron delocalization over the entire C–N–N–Ph linkage and accompanying resonance enhancement of the surface-bound adduct. The technique permits investigation of GC surface chemistry in two related directions. First, the surface coverage of carbonyls resulting from various pretreatments can be compared and related to kinetic behavior. It is likely that surface carbonyl density significantly affects the kinetics of a variety of redox processes at carbon electrodes.^{2,9} Second, analysis of vibrational modes, particularly in the 1500–1600 cm^{-1} region, will be used to deduce the local environment of surface carbonyl groups, with the intent of structurally defining surface carbonyl sites. The results of these investigations will be reported separately.

ACKNOWLEDGMENT

This work was supported by the Surface and Analytical Division of the National Science Foundation and an Amoco Industrial Fellowship to M.A.F. The suggestions of Olivier Schueller on DNPH chemistry were very valuable, as were the comments of the reviewers.

Received for review June 30, 1994. Accepted December 16, 1994.[®]

AC9406625

[®] Abstract published in *Advance ACS Abstracts*, January 15, 1995.